Bragg spectroscopy with an accelerating Bose-Einstein condensate

R. Geursen,* N. R. Thomas, and A. C. Wilson
Department of Physics, University of Otago, P.O. Box 56, Dunedin, New Zealand
(Received 9 July 2003; published 9 October 2003)

We present the results of Bragg spectroscopy performed on an accelerating Bose-Einstein condensate. The Bose-Einstein condensate undergoes circular micromotion in a magnetic time-averaged orbiting potential trap and the effect of this motion on the Bragg spectrum is analyzed. A simple frequency modulation model is used to interpret the observed complex structure, and broadening effects are considered using numerical solutions to the Gross-Pitaevskii equation.

DOI: 10.1103/PhysRevA.68.043611 PACS number(s): 03.75.Kk, 03.75.Nt, 32.80.Cy

I. INTRODUCTION

The experimental realization of a dilute Bose-Einstein condensate, a quantum-degenerate atomic Bose gas, has led to a wide range of experiments in atom optics (see, for example, Refs. [1,2]). The macroscopically occupied ground state exhibits large-scale coherence, which can be exploited in atom-optical techniques. One such technique is Bragg scattering, which has been applied to make precise measurements of condensate momentum [3,4], investigate excitations [5], measure the phase-coherence length [6], excite phonons [7], and to implement four-wave mixing [8] and a Mach-Zehnder interferometer [9]. More recently, Blakie *et al.* showed that the velocity sensitivity of Bragg scattering can provide a means of detecting superfluid flow associated with condensates in a vortex state [10]. In all this work, the initial Bose-Einstein condensates have been well described as wave functions with a stationary center of mass making them an ideal source for atom-optic experiments using Bragg scattering.

In conventional Bragg spectroscopy the spectrum is given by the spectral response function of the condensate [4], which is related to the momentum distribution and under certain conditions is a good measure of this distribution. In this work, we show that for an accelerating condensate, the spectrum is no longer a direct representation of the momentum distribution. We investigate Bragg spectroscopy for the case of a Bose-Einstein condensate undergoing circular micromotion in a time-averaged orbiting potential (TOP) trap [11,12]. Although the condensate micromotion is small in amplitude, we demonstrate that the center-of-mass acceleration can be large enough to dramatically alter the Bragg spectrum. Our experimental results are compared to a theoretical spectrum for the corresponding stationary condensate, illustrating that the effect of the acceleration is to significantly broaden the Bragg spectrum and introduce complex structure. We describe two simple models to explain the underlying physics of the observed behavior, and present numerical simulations using the one-dimensional Gross-Pitaevskii equation (GPE) which confirm our interpretation.

*Electronic address: reece@physics.otago.ac.nz

II. CONDENSATE MICROMOTION AND BRAGG SPECTROSCOPY

In this section we summarize aspects of micromotion in a TOP trap that are relevant to its affect on Bragg spectroscopy, and present two simple models for describing the modified Bragg scattering process.

The instantaneous magnetic field for our TOP trap is, as given in Ref. [12],

$$\mathbf{B}=[B_q'x+B_T\cos(\omega_T t)]\hat{\mathbf{i}}+[B_q'y+B_T\sin(\omega_T t)]\hat{\mathbf{j}}-2B_q'z\hat{\mathbf{k}}, \tag{1}$$

where B_q' is the quadrupole field gradient along the radial direction, B_T is the magnitude of the rotating bias field, and ω_T is the angular frequency of the the bias field rotation. Petrich *et al.* [12] showed that, for time scales longer than the rotation period, the atoms experience only the leading terms in the magnitude of the time-averaged magnetic field so that

$$B_{\mathrm{av}}\simeq B_T+\frac{B_q'^2}{4B_T}(r^2+8z^2), \tag{2}$$

where r is the radial coordinate. For many experiments, this time average is an appropriate description, but for Bragg spectroscopy this is not always the case [13]. The time-varying force on the condensate results in center-of-mass oscillation or micromotion (as pointed out by Petrich *et al.* [12]), to which Bragg spectroscopy is sensitive. The origin of this micromotion can be seen by considering the instantaneous potential of the TOP trap,

$$\begin{aligned}U(x,y,z,t)&=\mu|\mathbf{B}|\\&=\mu B_q'\{r_0^2+x^2+y^2+4z^2+2r_0[x\cos(\omega_T t)\\&\quad+y\sin(\omega_T t)]\}^{1/2},\end{aligned} \tag{3}$$

where $r_0=B_T/B_q'$ is the so-called "circle of death" radius (the radius where the $B=0$ point rotates in the $z=0$ plane) and the time-varying force is given by $\mathbf{F}(x,y,z,t)=-\boldsymbol{\nabla}U$. Typically, in the region of the condensate in the trap, $r_0 \gg x,y$ and we can approximate the magnitude of the force along the x axis (for example) as

$$F(t)\simeq-\mu B_q'\cos(\omega_T t). \tag{4}$$

Ignoring condensate mean-field effects (since the trapping force is large) we find that the classical solution for the magnitude of the time-varying center-of-mass momentum and position are given by

$$p(t)=\frac{-\mu B_q'}{\omega_T}\sin(\omega_T t), \tag{5}$$

$$x(t)=\frac{\mu B_q'}{m\omega_T^2}\cos(\omega_T t), \tag{6}$$

where m is the atomic mass and we have assumed for simplicity $p(0)=0$ and $x(0)=\mu B_q'/m\omega_T^2$. The condensate center-of-mass along the x axis performs simple harmonic motion, and from trap symmetry we deduce that the condensate performs circular motion in the plane of the rotating bias field. This result was first obtained and experimentally confirmed by Müller *et al.* [11].

To discuss the implications of centripetal acceleration for Bragg spectroscopy we first summarize Bragg scattering [14]. A moving optical grating is applied to the condensate and atoms can absorb n photons from one beam $(\omega_1,\mathbf{k}_1)$ and emit n photons, via stimulated emission, into the other $(\omega_2,\mathbf{k}_2)$, where $|\mathbf{k}_1|=|\mathbf{k}_2|=k=2\pi/\lambda$, and the detuning is $\delta=\omega_1-\omega_2$. This results in the transfer of momentum $\hbar|\mathbf{q}|=nP_{\mathrm{recoil}}\equiv 2n\hbar k\sin(\theta/2)$ and energy $\hbar n\delta$, where $\mathbf{q}=\mathbf{k}_1-\mathbf{k}_2$ and θ is the angle between the two beams forming the grating. This process will be resonant for noninteracting stationary atoms if the final kinetic energy of the atom is equal to the energy difference between the Bragg beams, i.e., $\hbar n\delta=(nP_{\mathrm{recoil}})^2/2m$.

When calculating the resonance condition for atoms which are initially moving in the laboratory frame an additional term arises, which can be attributed to the Doppler effect, and which we will call the Doppler term $\hbar\mathbf{P}\cdot\mathbf{q}/m$ (where $\mathbf{P}$ is the condensate momentum). In the micromotion case we have $\mathbf{P}=p(t)\hat{\mathbf{i}}$, giving a Doppler term which results in a new time-dependent Bragg detuning condition. For first-order Bragg scattering $(n=1)$ this condition is

$$\hbar\delta=\frac{P_{\mathrm{recoil}}^2}{2m}-\frac{\hbar|\mathbf{q}|\mu B_q'}{m\omega_T}\sin(\omega_T t). \tag{7}$$

Note that when δ is greater than $P_{\mathrm{recoil}}^2/2m\hbar$ the resonance condition can only be satisfied for $\sin(\omega_T t)<0$, so that Bragg scattering is resonant only for some instant during half of the TOP cycle. Similarly, if $\delta<P_{\mathrm{recoil}}^2/2m\hbar$, resonance only occurs if $\sin(\omega_T t)>0$. Therefore, if the Bragg pulse length T_B is not an integer multiple of the TOP period, the Bragg spectrum will be asymmetric. We avoid this problem by having T_B equal to eight TOP rotations.

Alternatively, we can picture the Bragg scattering process in the rest frame of the condensate and think of the micromotion as modifying the optical potential. In the absence of micromotion the effective optical potential from two counterpropagating, pulsed, laser beams is given by [15]

$$V_{\mathrm{opt}}(x,t)=\hbar V(t)\cos(|\mathbf{q}|x-\delta t), \tag{8}$$

where the amplitude $\hbar V(t)$ is twice the ac Stark shift at the grating maximum. In this case, the potential has a spectrum centered at the frequency difference between the two Bragg beams, with an rms half-width $\Delta\nu_{T_B}\simeq 1/(2T_B)$.

The effect of the micromotion can be incorporated into the optical potential by transforming to the stationary frame of the condensate. The resulting time-dependent frequency shift of the Bragg resonance condition in the laboratory frame produces a frequency modulated (FM) optical potential in the condensate rest frame, as pointed out by Cristiani *et al.* [13]. The modified potential becomes

$$\overline{V}_{\mathrm{opt}}(x,t)=\hbar V(t)\cos[|\mathbf{q}|x-\delta t-|\mathbf{q}|A\cos(\omega_T t)], \tag{9}$$

where the bar denotes the center-of-mass frame of the condensate and $A=\mu B_q'/m\omega_T^2$. This frequency modulation generates sidebands in the frequency spectrum of the optical potential, yielding multiple first-order Bragg resonances.

Bragg spectroscopy involves scanning the frequency difference δ through resonance and measuring the out-coupled condensate fraction. To resolve features in the condensate's Bragg spectrum requires the frequency width of the Bragg light to be narrower than the spectral width of the feature. Mechanisms that contribute to the condensate momentum width [3,4] are Doppler broadening $\Delta\nu_D=\sqrt{(21/8)}\times(P_{\mathrm{recoil}}/2\pi mR)$, where R is the condensate radius, and mean-field (collisional) broadening $\Delta\nu_n=\sqrt{(8/147)}\times(\mu_{\max}/h)$, where $\mu_{\max}$ is the chemical potential at the peak density. In addition to these effects and the spectral broadening associated with finite pulse time, there is also a power-broadening contribution $\Delta\nu_p\simeq kV/\pi|\mathbf{q}|$ [15].

III. EXPERIMENTAL DETAILS

Our apparatus for producing Bose-Einstein condensates is described in Ref. [16], but with some minor modifications. Briefly, we use a double magneto-optical trap (MOT) to cool and trap ^{87}Rb atoms, which is driven by injection-seeded diode lasers and with continuous loading of the low-pressure MOT. The laser cooled sample is transferred to a magnetic TOP trap and evaporatively cooled to produce a condensate containing $\approx 2\times 10^4$ atoms in the $|F=2,m_F=2\rangle$ state.

Following condensate formation, the magnetic trap was adiabatically relaxed (by reducing the quadrupole field gradient and increasing the bias field over 200 ms) to trapping frequencies of $\omega_{\mathrm{radial}}=\omega_z/\sqrt{8}=2\pi\times 18$ Hz. For our bias field rotation frequency $\omega_T=2\pi\times 2.78$ kHz, the corresponding tangential micromotion velocity is 3.3 mm s^{-1} (compared to the two-photon recoil velocity of 11.8 mm s^{-1}) . Although the amplitude of the motion is only 190 nm, the high relative velocity means that the effect of the micromotion on the Bragg spectrum is substantial.

Counterpropagating Bragg beams were generated using a Ti:sapphire laser, the output of which was split and passed through two acousto-optic modulators to provide individual frequency control. We used a detuning $\Delta\simeq 2\pi\times 4.49$ GHz above the $^5S_{1/2}F=2$ to $^5P_{3/2}F'=3$ transition, giving a spon-

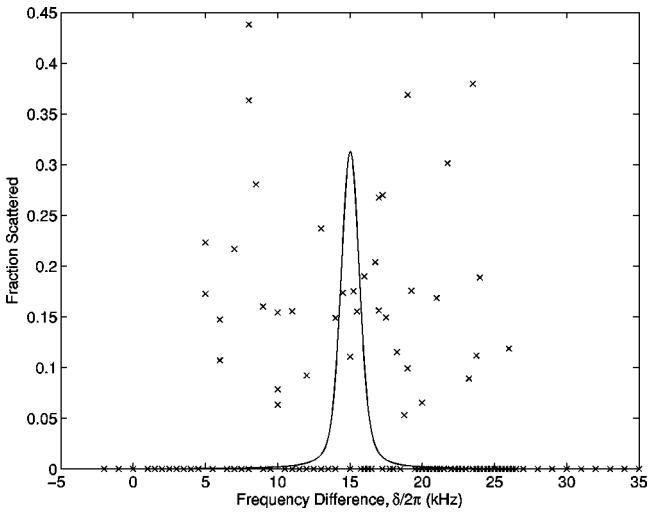

FIG. 1. Bragg scattered data for a Bose-Einstein condensate accelerating due to micromotion in a TOP trap (crosses), together with a numerical simulation using the linear one-dimensional (1D) Gross-Pitaevskii equation assuming no micromotion (solid line). Results are for $B_q' = 90\ \mathrm{G\,cm^{-1}}$ (corresponding to a maximum center-of-mass velocity of $3.3\ \mathrm{mm\,s^{-1}}$) and an intensity of $0.26(5)\ \mathrm{mW\,cm^{-2}}$ [corresponding to a power-broadening contribution of 0.22(4) kHz].

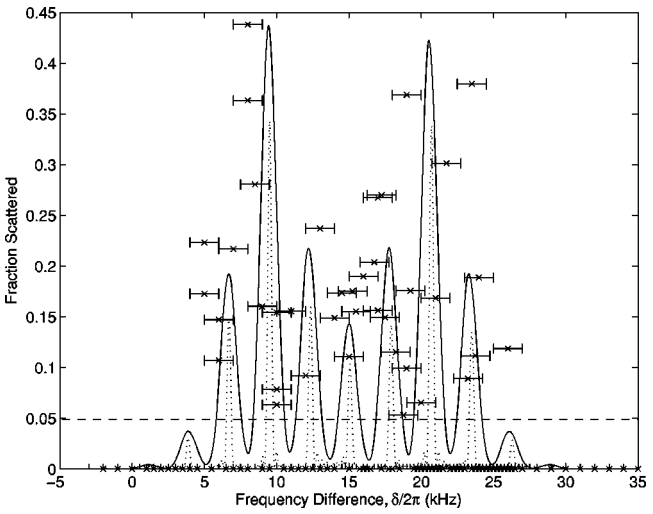

FIG. 2. The Bragg scattered data from Fig. 1 (crosses), together with the spectrum of the Bragg light (dotted line) and the corresponding numerical simulation (solid line) using the linear 1D Gross-Pitaevskii equation. The relative heights of the peaks in the FM spectrum are determined by the modulation index and the width of each peak is determined by the finite pulse length T_B. Each data point has an uncertainty in the scattered fraction of $\pm$ 0.1. The dashed line indicates the minimum detectable fraction for these data and below this limit we plot the data as having zero scattered fraction.

taneous scattering rate of $\approx 5\ \mathrm{s^{-1}}$ (i.e., negligible for our purposes). Both beams were aligned in the plane of the rotating bias field. A pulse length of $T_B = 2.88$ ms was chosen for a spectral width $\Delta\nu_{T_B}$ comparable to the width of an equivalent stationary condensate with our parameters. The pulse length is also shorter than a quarter trap period so that the Bragg scattered fraction becomes well separated from the unscattered component in time of flight. The intensity was set to either 0.26(5) or $0.6(1)\ \mathrm{mW\,cm^{-2}}$. To minimize the effect of timing differences between consecutive measurements we synchronized the Bragg pulse with the rotation of the bias field. At the end of the pulse, the condensate was released from the trap and imaged by resonant absorption after 9 ms of free expansion. Bragg spectroscopy was performed by measuring the first-order scattered fraction as a function of the frequency difference between the two Bragg beams.

IV. RESULTS AND DISCUSSION

For a stationary Bose-Einstein condensate confined in a static harmonic potential with our experimental parameters, the Bragg spectrum has a simple form (essentially Gaussian) with a narrow width. However, the presence of micromotion introduces substantial broadening and complex structure. In Fig. 1 we show the Bragg scattered data obtained for a condensate undergoing centripetal acceleration in the plane of the Bragg beams. Also shown is a theoretical spectrum for our condensate parameters, ignoring mean-field effects (which are small in this case) and assuming no micromotion. The rms half-width of the theoretical curve is 0.56 kHz, which is consistent with our measurements made in time of flight where micromotion is absent.

To explain the complex structure in the experimental spectrum, we now present results of the simple FM picture described in the preceding section.

We obtain the frequency components present in the Bragg light by performing a Fourier transform on the modified optical potential given by Eq. (9). The result is a spectrum for the Bragg light which has a carrier at the frequency difference between the Bragg beams (δ), and sidebands (spaced by ω_T) with relative amplitudes determined by Bessel functions of the FM spectrum [17]. In this case the modulation index, upon which the Bessel functions are strictly dependent, is just the maximum Doppler shift divided by the modulation frequency and can therefore be adjusted by simply changing the quadrupole field gradient. In Fig. 2 the experimental data from Fig. 1 is overlaid with the corresponding frequency spectrum of the modified optical potential $\overline{V}_{\mathrm{opt}}$ (scaled by an arbitrary factor). Since there are a number of sidebands with significant amplitude, when we sweep the carrier frequency (δ) to generate the Bragg spectrum we bring successive sidebands into resonance with the condensate. The exact form of the Bragg spectrum is then a combination of the complex spectral character of the light and the spectral response of the stationary condensate. When the Bragg spectrum of the stationary condensate is narrow compared to the bias field rotation frequency (as in our case), the Bragg spectrum with micromotion has peaks at frequencies corresponding to the locations of the sidebands. To within the spectral uncertainty of our Bragg experiments, $\approx \pm 1$ kHz, this behavior is shown in the data of Fig. 2. Although we cannot resolve the predicted individual spectral peaks, the overall range of frequencies for which we get

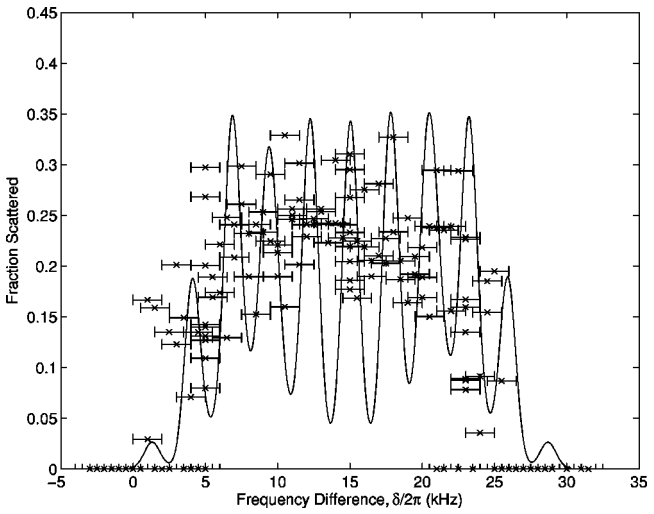

FIG. 3. Power-broadened Bragg scattered data (crosses) and the corresponding 1D linear GPE simulation (solid line). Experimental parameters are $B'_q = 90\ \mathrm{G\,cm^{-1}}$ and an intensity of $0.6(1)\ \mathrm{mW\,cm^{-2}}$ [corresponding to a power-broadened contribution of 0.5(1) kHz]. Each data point has an uncertainty in the scattered fraction of between ± 0.05 and $\pm\ 0.09$ depending on $\delta/2\pi$.

Bragg scattering matches the range over which there is significant sideband intensity. Our spectral resolution is limited by a number of physical processes, including the mechanical stability of the optics and the electrical stability of the currents driving the magnetic trap. From a heterodyne measurement using the two Bragg beams we determined that the uncertainty due to the mechanical stability of the optics (which Doppler shifts the light) is $\approx \pm 0.4$ kHz, whereas the contribution to the uncertainty from current stability is $\approx \pm 0.6$ kHz. The main effect of current instability is to put noise on the quadrupole gradient, which in turn puts noise on the time-varying center-of-mass momentum, as can be seen from Eq. (5). The uncertainties in our measurements of the fraction of scattered atoms were determined by making repetitive measurements with the same parameters, and can vary across the spectrum. The significant contributions arise from shot-to-shot condensate variation and the minimum scattered fraction we can measure with our imaging system.

At low intensity the simple FM picture predicts some important features such as the frequencies and relative heights of the peaks, but the widths of each peak only include a contribution from the finite pulse time. To obtain a more accurate prediction of the experimental results we include the dynamic term of the TOP trap in a collisionless one-dimensional Gross-Pitaevskii equation simulation, using a one-dimensional version of Eq. (3) as our magnetic potential. Results of this simulation are shown as the solid line in Fig. 2, confirming aspects of the FM picture and providing better agreement with the data.

As an additional test of our interpretation we now consider a power-broadened case [i.e., a higher value for $V(t)$]. This alleviates the need to resolve very narrow spectral features and gives larger (more easily measured) Bragg scattered fractions near the central region of the spectrum. Figure 3 shows a power-broadened Bragg spectrum together with the corresponding numerical simulation. The contribution to the condensate width from power broadening is 0.5(1) kHz, compared to 0.26 kHz from Doppler broadening (the dominant condensate contribution). Within the limits of our experimental uncertainty, the agreement between the data and the simulation is reasonable. The overall width of the spectrum is well predicted, and the variation in the Bragg scattered fraction is reduced, as expected. The small difference between the center frequencies of the GPE simulations and experimental data spectra is likely to be due to our linear one-dimensional modeling of a nonlinear three-dimensional experiment [4,15,18]. The slight asymmetry in the numerical spectrum (which we cannot resolve in the experimental data) becomes apparent when transforming to the condensate rest frame through a damped drift term [19]. Additional asymmetry can occur if the Bragg pulse length does not match an integer multiple of the TOP trap rotation period, but this is not the case for the results presented here.

A process not included in our linear GPE simulations, but which can significantly alter the Bragg spectrum [15], is the mean-field collisional interaction in the condensate. A detailed theoretical treatment is currently being prepared [19].

V. CONCLUSIONS

We have presented experimental results and a simple theoretical analysis of Bragg spectroscopy performed on an accelerating Bose-Einstein condensate. This work extends Bragg scattering experiments beyond those involving Bose-Einstein condensates with a stationary (or constant velocity) center of mass. Using condensate micromotion in a magnetic TOP trap, we have shown that for circular center-of-mass motion the Bragg spectrum is modified significantly from a simple momentum interpretation. An analysis which treats the angular acceleration as equivalent to frequency modulating the optical grating provides a useful interpretation for the complex structure we observe in the Bragg spectra. Numerical simulations using the one-dimensional linear Gross-Pitaevskii equation extend the analysis to include other broadening mechanisms. Although we are not able to resolve the narrow features predicted by our models, the overall spectral width and scattered fractions are in quantitative agreement with the theoretical results, confirming our simple physical interpretation. However, a more comprehensive theoretical description of Bragg spectroscopy with accelerating Bose-Einstein condensates is needed to characterize the effects of collisions and collective excitations in higher dimensions.

ACKNOWLEDGMENTS

The authors thank K. J. Challis for assistance with computational and theoretical work, G. Duffy for help with data acquisition, and R. J. Ballagh for useful comments and suggestions. We gratefully acknowledge the financial support of the Royal Society of New Zealand Marsden Fund (Contract No. UOO508).

[1] P. Meystre, *Atom Optics* (Springer-Verlag, New York, 2001).
[2] J.R. Anglin and W. Ketterle, Nature (London) **416**, 211 (2002).
[3] J. Stenger, S. Inouye, A.P. Chikkatur, D.M. Stamper-Kurn, D.E. Pritchard, and W. Ketterle, Phys. Rev. Lett. **82**, 4569 (1999).
[4] P.B. Blakie, R.J. Ballagh, and C.W. Gardiner, Phys. Rev. A **65**, 033602 (2002).
[5] J. Steinhauer, R. Ozeri, N. Katz, and N. Davidson, Phys. Rev. Lett. **88**, 120407 (2002).
[6] F. Gerbier, S. Richard, J.H. Thywissen, M. Hugbart, P. Bouyer, and A. Aspect, e-print cond-mat/0210206.
[7] D.M. Stamper-Kurn, A.P. Chikkatur, A. Görlitz, S. Inouye, S. Gupta, D.E. Pritchard, and W. Ketterle, Phys. Rev. Lett. **83**, 2876 (1999).
[8] J.M. Vogels, K. Xu, and W. Ketterle, Phys. Rev. Lett. **89**, 020401 (2002).
[9] Y. Torii, Y. Suzuki, M. Kozuma, T. Sugiura, T. Kuga, L. Deng, and E.W. Hagley, Phys. Rev. A **61**, 041602 (2000).
[10] P.B. Blakie and R.J. Ballagh, Phys. Rev. Lett. **86**, 3930 (2001).
[11] J.H. Müller, O. Morsch, D. Ciampini, M. Anderlini, R. Mannella, and E. Arimondo, Phys. Rev. Lett. **85**, 4454 (2000).
[12] W. Petrich, M.H. Anderson, J.R. Ensher, and E.A. Cornell, Phys. Rev. Lett. **74**, 3352 (1995).
[13] M. Cristiani, O. Morsch, J.H. Müller, D. Ciampini, and E. Arimondo, Phys. Rev. A **65**, 063612 (2002).
[14] M. Kozuma, L. Deng, E.W. Hagley, J. Wen, R. Lutwak, K. Helmerson, S.L. Rolston, and W.D. Phillips, Phys. Rev. Lett. **82**, 871 (1999).
[15] P.B. Blakie and R.J. Ballagh, J. Phys. B **33**, 3961 (2000).
[16] J.L. Martin, C.R. Mckenzie, N.R. Thomas, J.C. Sharpe, D.M. Warrrington, P.J. Manson, W.J. Sandle, and A.C. Wilson, J. Phys. B **32**, 3065 (1999).
[17] See, for example, J.M. Supplee, E.A. Whittaker, and W. Lenth, Appl. Opt. **33**, 6294 (1994).
[18] S. Morgan, S. Choi, K. Burnett, and M. Edwards, Phys. Rev. A **57**, 3818 (1998).
[19] K.J. Challis and R.J. Ballagh (private communication).